The Boardman Regional Flux Experiment

J. C. Doran,[1] F. J. Barnes,[2] R. L. Coulter,[3] T. L. Crawford,[4]
D. D. Baldocchi,[4] L. Balick,[5] D. R. Cook,[3] D. Cooper,[2] R. J. Dobosy,[4]
W. A. Dugas,[6] L. Fritschen,[7] R. L. Hart,[3] L. Hipps,[8] J. M. Hubbe,[1] W. Gao,[3]
R. Hicks,[6] R. R. Kirkham,[1] K. E. Kunkel,[9] T. J. Martin,[3] T. P. Meyers,[4] W. Porch,[2]
J. D. Shannon,[3] W. J. Shaw,[1] E. Swiatek,[8] C. D. Whiteman[1]

Abstract

A field campaign was carried out near Boardman, Oregon, to study the effects of subgrid-scale variability of sensible- and latent-heat fluxes on surface boundary-layer properties. The experiment involved three U.S. Department of Energy laboratories, one National Oceanic and Atmospheric Administration laboratory, and several universities. The experiment was conducted in a region of severe contrasts in adjacent surface types that accentuated the response of the atmosphere to variable surface forcing. Large values of sensible-heat flux and low values of latent-heat flux characterized a sagebrush steppe area; significantly smaller sensible-heat fluxes and much larger latent-heat fluxes were associated with extensive tracts of irrigated farmland to the north, east, and west of the steppe. Data were obtained from an array of surface flux stations, remote-sensing devices, an instrumented aircraft, and soil and vegetation measurements. The data will be used to address the problem of extrapolating from a limited number of local measurements to area-averaged values of fluxes suitable for use in global climate models.

1. Introduction

In recent years, the problem of characterizing turbulent fluxes of heat, momentum, and moisture over inhomogeneous surfaces has received increasing attention (e.g., Mahrt 1987; Avissar and Pielke 1989; Noilhan and Planton 1989; Claussen 1990; Rabin et al. 1990; Kustas et al. 1991). The issue is important not only in its own right but also because it has particular relevance to the performance of general circulation models (GCMs), in which a single grid element can encompass a variety of surface and topographical features. Specifying the proper surface fluxes of heat and moisture is critical because the sensible-heat flux is a major factor in determining the structure and evolution of the winds, temperatures, and depths of the boundary layer, while both heat and moisture fluxes affect the formation of clouds and the transfer of solar and thermal radiation through the atmosphere. The choice of a single flux value that is appropriate for such an element is not obvious, and the accuracy of a model forecast may be adversely affected by a poor choice. Moreover, the use of such models in forecasting short-term regional responses to long-term climate trends may be compromised if heterogeneity is not explicitly and correctly treated. Although programs such as HAPEX-MOBILHY (André et al. 1990), FIFE (Hall et al. 1990), and MONSOON 90 (Kustas et al. 1991) are recent sources of valuable information, there is still a relative scarcity of datasets collected specifically with this problem in mind.

Thus, in June 1991, a field campaign was conducted near Boardman, Oregon, to study the effects of subgrid-scale variability of surface sensible- and latent-heat fluxes on surface boundary-layer properties, and to provide data with which to address the problem of extrapolating from a limited number of local measurements to area-averaged values of fluxes suitable for use in GCMs. The experiment was conducted in a region of severe contrasts in adjacent surface types that accentuated the response of the atmosphere to variable surface forcing. The study was part of the U.S. Department of Energy's (DOE) Atmospheric Radiation Measurement (ARM) program (Department of Energy 1990). The principal aim of ARM is to improve the treatment of radiation and clouds in GCMs for use in climate studies, and one aspect of the program deals with the question of how to provide descriptions of subgrid-scale processes in GCMs. Researchers in the ARM program will carry out extensive tests of single-column GCMs requiring accurate values of

[1]Pacific Northwest Laboratory, Richland, Washington
[2]Los Alamos National Laboratory, Los Alamos, New Mexico
[3]Argonne National Laboratory, Argonne, Illinois
[4]Atmospheric Turbulence and Diffusion Division, Oak Ridge, Tennessee
[5]EG&G Measurements, Inc., Las Vegas, Nevada
[6]Blackland Research Center, Texas Agricultural Experiment Station, Temple, Texas
[7]University of Washington, Seattle, Washington
[8]Utah State University, Logan, Utah
[9]Illinois State Water Survey, Champaign, Illinois

surface fluxes over scales of 100 km or more for comparisons with model results. However, as noted above, the determination of these fluxes is difficult, and parameterizations used in GCMs are often based on simplifying assumptions that may have limited validity. The field campaign was thus designed with these issues in mind.

The objectives of the campaign included:

- evaluating methods of measuring fluxes over inhomogeneous surfaces;
- examining the variation of surface fluxes over a range of scales (< 1 km to > 10 km);
- identifying a clear signature in the boundary layer of the effects of inhomogeneities in surface sensible- and latent-heat fluxes;
- establishing procedures for extrapolating flux values from smaller scales to larger ones; and
- testing one or more parametric schemes relating turbulent fluxes to vertical gradients of mean quantities.

Participants in the campaign included researchers from DOE's Argonne National Laboratory, Los Alamos National Laboratory, and Pacific Northwest Laboratory; the National Oceanic and Atmospheric Administration's Atmospheric Turbulence and Diffusion Division; EG&G/Las Vegas; the Illinois State Water Survey; Blackland Research Center; the University of Utah; and the University of Washington.

In the following sections, a description of the site chosen for the field campaign is given, the instrumentation used and the measurements taken are described, the meteorological conditions during various phases of the experiment are summarized, examples of some preliminary results are provided, and the scope of additional planned analyses is outlined.

2. Experimental site

Typical GCM grid elements of order 100 km on a side include distributions of surfaces that range from apparently uniform composition to essentially random arrangements of disparate types. In order to simplify subsequent analyses, a site was sought that could be characterized by a relatively small number of different surfaces whose heat and moisture fluxes would differ markedly. Ideally, different surfaces would have scales of 10 km or more so that locally induced circulations or other significant modifications to the boundary-layer structure would have the opportunity to develop; moreover, the number of different surfaces should be limited so that the number of internal boundary layers would be small. To avoid complications from topographic effects, the site should also be flat or nearly so.

The site chosen for the experiment was located near Boardman, in northeastern Oregon, and is shown schematically in Fig. 1. A large, sagebrush steppe area is bordered on the east, northeast, and west by extensive areas of irrigated farmland. The terrain is generally flat to gently rolling with a slight tilt toward higher elevations to the south; some deeper gullies can be found along streambeds in the western part of the domain. The terrain rises approximately 150 m from the Columbia River in the north to the southern boundary in the figure, with an average slope of 0.75%. The prevailing winds are from the west-southwest; such winds traverse extended areas of alternating steppe and farmland. To a first approximation, the area can be considered to consist of two principal land types—hot, dry steppe and cool, moist farmland. The scales of each of these two surfaces are sufficiently large that, under favorable conditions, noticeable modifications in the boundary-layer structure should be observable as the winds blow from one region to the other.

Preliminary qualitative surveys of the steppe site showed that one grass and two shrub associations were most important in the spatial coverage of the transect area in the northern portion of the site. The grassland areas were dominated by needle-and-thread (Stipa comata), a perennial bunchgrass. One site was severely overgrazed and dominated by an annual grass, cheatgrass (Bromus tectorum), with needle-and-thread as a subdominant component. Aboveground green vegetative cover on the grassland sites ranged from 20% to 40%. Biomass estimates for three sites in this community ranged from 13 to 55 g m^{-2}. The two shrub communities were dominated either by rabbitbrush (Chrysothamnus nauseosus) or bitterbrush (Purshia tridentata), with understories of needle-and-thread and/or cheatgrass. Overstory canopy cover on the shrub sites was about 14%. At the time of the study, the perennial grasses had largely completed vegetative growth and were starting to seed, while the annual grasses were senescent, with no green foliage evident. The shrubs were still in an active vegetative growth phase.

Conditions across the steppe were dry at the time of the measurement campaign. Gravimetric soil-moisture determinations were made from composites of three samples at each site, and two sets of measurements were taken 10–14 days apart. Soil moisture from 0- to 15-cm depth ranged from 1.1% to 4.1% volume, and from 2.5% to 6.4% volume in the 15- to 30-cm-depth samples. During the course of the experiment no major trends in moisture content were found.

The farmland is watered by center-pivot irrigation

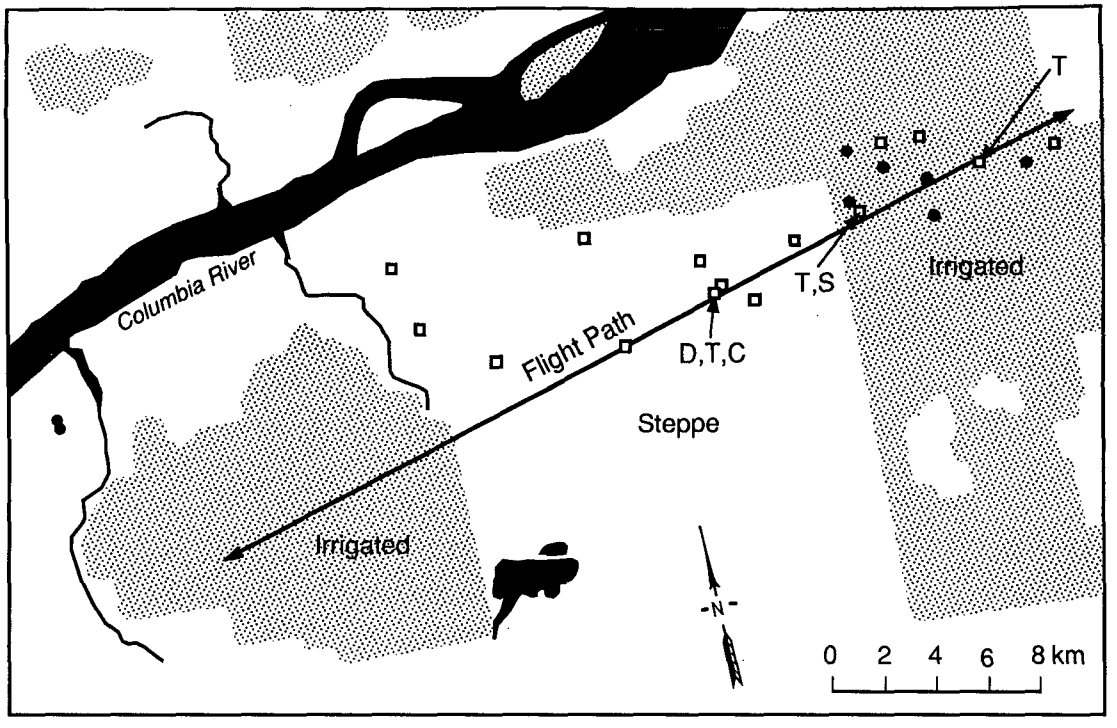

FIG. 1. Schematic diagram of experimental area. Black areas are bodies of water, stippled areas are irrigated farmland, and the remaining area is steppe. Squares are eddy-correlation instruments, circles are Bowen-ratio energy balance stations, D denotes three-component Doppler sodar, T marks locations of tethered-balloon launches, C is the location for the convergence measurements, and S shows location of minisodars for measurements of internal boundary-layer development. The primary flight path for the instrumented aircraft is also shown.

systems and features four principal crops: alfalfa, corn, wheat, and potatoes. The stippled areas in Fig. 1 contain ~500 separate fields; most are circular and have a diameter of approximately 800 m. The circles are generally arranged either in square or hexagonal patterns, thereby covering ~75%–90% of the stippled areas in the figure. The remaining land in these areas consists primarily of dirt roads and open space between fields; the open spaces were usually planted with vegetation to reduce blowing dust.

3. Instrumentation and measurements

The distribution of surface flux measurements shown in Fig. 1 provided extensive coverage of both the semiarid and wetter regions over a path approximately 40 km long and 6 km wide. Surface fluxes of sensible and latent heat were measured using eddy-correlation instruments and Bowen-ratio energy balance stations. Both one- and three-component sonic anemometers with fast-response temperature sensors were used for determining sensible-heat fluxes. The temperature sensors were either thermocouples, microbead thermistors, or platinum wire resistance elements; in two of the instruments, virtual temperature fluctuations were determined directly from the measurement of the speed of sound by the sonic anemometers. Most of the eddy-correlation instruments were also equipped with fast-response UV or IR hygrometers (Auble and Meyers 1992) for measuring latent-heat fluxes.

A qualitative analysis across the steppe revealed three primary plant communities in the measurement area; ten eddy-correlation devices were distributed in the steppe to sample conditions within these communities. Five additional eddy-correlation sites were located in the farm area on the downwind sides of fields containing the four principal crop types. At one of the farm sites, approximately 800 m east of the boundary between dry and moist terrain, eddy-correlation measurements were taken at two heights (4 and 12 m) to measure the extent of flux divergence in the developing boundary layer. Measurement heights for other eddy-correlation instruments ranged from 3 to 4 m. Bowen-ratio energy balance stations were located at six additional sites in the irrigated area and at one site in the steppe region.

Airborne measurements were obtained by flying a mobile flux platform (Crawford et al. 1990) on a single-engine aircraft for a total of 93 h of measurements over the course of the experiment. This platform measured

mean wind speed and direction, temperature, and humidity; turbulent fluctuations of wind speed, temperature, moisture, O_3, and CO_2; and ground radiating temperatures. These measurements will be used in several ways: 1) to test the feasibility of using the airborne flux measurements of sensible and latent heat to obtain effective "line-averaged" flux values over the steppe and over the farmland, so that these values can then be compared with averages calculated from some weighted summation of fluxes measured by the surface stations; 2) to study differences in the structure and circulations in the boundary layer caused by the sharply contrasting properties of the underlying surfaces; and 3) to test parameterization schemes that relate sensible-heat fluxes to ground–air temperature differences, by combining measurements of ground and surface temperatures, wind speeds at flight altitude, and fluxes of sensible heat. Such schemes are similar to those used in GCMs.

Previous studies have shown that topography, soil type and moisture content, vegetative biomass, and vegetative activity are closely related to fluxes of heat and moisture.

The most commonly flown path was along the line of ground-based flux instruments shown in Fig. 1. These sampling paths were supplemented by additional patterns, including "asterisks" over both wet and dry areas, flights perpendicular to the principal flight path, and deep soundings through the depth of the boundary layer. Each asterisk pattern consisted of a series of 10-km segments, with eight different headings evenly spaced through 360° and centered on a common point, and were designed to study the degree of horizontal homogeneity over the steppe and the farm areas. For flight paths along the line of ground-based instruments, there was a further division of sampling patterns. The principal pattern was a series of sampling runs over a given path and fixed altitude. By combining the results from corresponding sections of each path, we hope to increase the statistical significance of the flux measurements over the two principal surface types in the sampling area. This pattern was occasionally modified to include a series of flights along the same path but at various altitudes to measure the extent of vertical flux divergence. Flight speeds were approximately 50 m s^{-1} and typical sampling altitudes ranged from approximately 10 to 200 m AGL (above ground level).

Previous studies have shown that topography, soil type and moisture content, vegetative biomass, and vegetative activity are closely related to fluxes of heat and moisture. To establish such relationships for this experiment, soil and vegetation analyses in both the agricultural area and the steppe regions were carried out prior to and in conjunction with the flux measurements (Barnes et al. 1992). The finescale variability in surface soil moisture (0–30-cm depth) was determined from 40 time domain reflectometry (TDR) measurements around a steppe site during three days of a supplementary experiment on small-scale variations of surface fluxes. TDR measurements (number of samples n = 4) of soil moisture at three steppe sites were taken every 1–3 days throughout the experiment. TDR measurements (n = 1 to 3) at an additional six sites were taken two days before and immediately following a rainstorm that deposited 0.2 to 1.4 cm across the steppe (mean 0.7 cm, n = 9). Gravimetric soil-moisture samples (three samples composited into two depths, 0–15 and 15–30 cm) were taken at most sites at the start and end of the experimental period.

In the agricultural area, periodic soil-moisture determinations were made in fields of wheat and corn. Latent- and sensible-heat flux, soil-heat flux, and net radiation-balance measurements were made at the same locations. Daily soil-moisture measurements (0–30 cm), using grids of time domain reflectometry probes (n = 15), were also made over about one-week periods in each of four fields (alfalfa, corn, potatoes, and wheat) that were instrumented with Bowen-ratio stations. Gravimetric soil samples (composites of three samples) were taken at one or two times from three fields—potatoes, corn, and wheat. The CO_2 flux measurements over two crops (wheat and corn) were made with a tower-mounted CO_2 eddy-correlation system. The source–sink potential for CO_2 and water vapor in the plant canopies in these fields was quantified by measurements of stomatal conductance and leaf-area indices. Distribution of the irrigation input along the pivot arm of the irrigation system and soil bulk density were determined for the fields under study. Leaf-area indices and/or biomass estimates for the study fields were made using both harvest techniques and light interception studies.

Some features of the boundary-layer structure were determined through a combination of aircraft measurements, tethered balloons, and sodars. The aircraft made two or more vertical soundings through the boundary layer on each flight day to obtain mean wind, temperature, and moisture profiles. A three-axis sodar located in the steppe region provided mean wind speeds up to heights of 600 m. On five days, tethered balloons were flown at three sites to measure profiles of wind velocity and wet- and dry-bulb temperatures to depths of ~1 km. The three sites were a steppe site

(site DTC in Fig. 1), a farm site approximately 6.5 km east of the boundary between the steppe and the farm, and a second farm site about 800 m east of the boundary. This arrangement was designed to allow measurements in well-developed boundary layers over both the steppe and farm; for westerly winds, the transition zone between the steppe and farm could also be studied.

One of the revealing indicators of the effects of contrasting surface characteristics is the vertical profile of the temperature structure parameter, C_T^2 (e.g., Stull 1988). In unstable conditions it is a function of the surface sensible-heat flux (H) and the height above the surface; with increasing stability it becomes dependent upon stress. The vertical profiles of C_T^2 derived from analysis of the acoustic signals reveals boundary-layer growth and development, temporally through their individual evolutions and spatially through comparative profiles from different sites. The near-surface portion of the profile is characteristic of H on the local scale, while higher portions of the profile reflect H over increasingly larger areas.

One of the revealing indicators of the effects of contrasting surface characteristics is the vertical profile of the temperature structure parameter, C_T^2.

Vertical profiles of C_T^2 were measured by vertically oriented sodars and minisodars located near the dry–wet transition zone. Three axes of a minisodar were separated by 100 m in a line along the prevailing wind direction. This linear array was operated in both corn and potato fields just downwind of the discontinuity between the steppe and the irrigated farmland. A single-axis minisodar was operated primarily within the steppe region, both to characterize the steppe conditions and to provide vertical-velocity estimates in conjunction with a convergence experiment described below. A conventional, vertically pointing sodar was located downwind of the irrigated corn field. These instruments also provided a measure of the boundary-layer growth and development through the lowest 500 m.

Two optical arrays were deployed to obtain line averages of C_n^2, the refractive index structure function. One array, using laser path-averaging anemometers, was located in the vicinity of the three-axis minisodar array (Coulter et al. 1992). It had paths approximately 200 m in length and 2 to 3 m high, across fields of potatoes, corn, and a corn–potato boundary. The other array employed both laser path-averaging and infrared large optic saturation-resistant crosswind and optical turbulence sensors, arranged in a triangle with legs also about 200 m long and 2 m high; this array was located in a steppe site (Porch et al. 1992). The principal component of C_n^2 is C_T^2, which can be related to heat flux in the same way as the sodar measured values (Wyngaard and Clifford 1978). In this case, the line averages of C_T^2 at a single height are directly related to the heat fluxes from surfaces beneath them and immediately upwind. The spatially averaged winds determined from the triangular array were used to measure the local convergence or divergence of the horizontal winds. A cup-and-vane anemometer was also located at each corner of the array to provide another estimate of these quantities. A minisodar collocated at this site allowed the convergence or divergence to be related to the vertical wind speeds over the triangle.

On two days during the experiment, a Convair 580 aircraft was used to acquire images over the farm and steppe sites, using a multispectral scanner and two aerial mapping cameras. The multispectral scanner had a 2.5-mrad instantaneous field of view and acquired images at ten visible, near-, and middle-infrared bands, and at two gains in the thermal infrared. The cameras were equipped with 6- and 12-inch lenses and both Aerocolor and color-infrared film, depending on the objectives during each flight line. Detailed mapping of vegetation will be possible over some of the steppe transects using these data. Sensible-heat flux measurements from a supplementary small-scale flux study at the steppe site will be correlated with the thermal data from the same location.

4. Schedule and meteorological conditions

During an instrument comparison exercise on 31 May and 1 June, the wind speeds were quite light and exceeded 2 m s^{-1} only toward the end of the comparison. Skies were clear throughout the period. Following this exercise, approximately half of the flux-measurement instruments were located at the sites shown in Fig. 1. The other half were placed in the steppe in a relatively small area, several hundred meters on a side, to examine the small-scale variability of fluxes over a semiarid region. These measurements were taken on 2–5 June, a period characterized by moderate winds (~10 m s^{-1}) and clear skies initially, followed by decreasing winds and increasing clouds. The instruments used in the small-scale study were then moved to their final positions in the steppe area, where they remained until the conclusion of the experiment on 19 June.

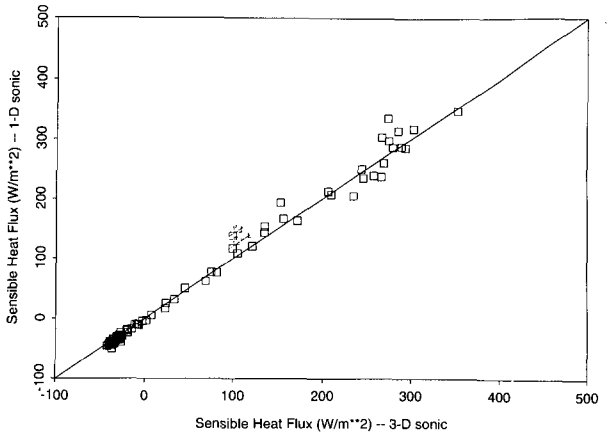

FIG. 2. Comparison of sensible-heat fluxes measured with three-component and single-component sonic anemometer systems. The former system also measured fluctuations in virtual temperature, while the latter system obtained temperature fluctuations with a thermocouple. The solid line represents perfect agreement between the systems.

Although wind directions during this campaign were predominantly from the west-southwest, as anticipated, wind speeds were often higher than had been hoped; on one day, sustained surface winds of 15–20 m s^{-1} were experienced. High wind speeds occasionally prevented the instrumented tethered balloons from being flown. With low wind speeds, contrasts between the boundary layers over the steppe and farm areas would be expected to be most pronounced, and locally induced circulations would be most evident. In contrast, with higher speeds advective effects become more important. In addition, when winds were lighter, wind directions became more variable, and some flux measurements over the farm sites may have been compromised because of poor fetch conditions. Nevertheless, data from over half of the days appear potentially useful for analyses.

5. Results

Prior to the intensive measurement period of the experiment, a comparison of the various instruments' performance (eddy-correlation and Bowen-ratio stations) was carried out for approximately 24 h in a recently cut alfalfa field. The sonic anemometers were positioned along a line approximately 15 m long, while the Bowen-ratio stations lay along an arc approximately 100 m long starting about 50 m from the sonic anemometer's line. Analyses of data collected during this period are continuing, but preliminary results show generally good agreement among the various instruments. An example is given in Fig. 2, which shows a comparison of the sensible-heat fluxes obtained from two different sonic-anemometer configurations. In one arrangement, a three-component sonic anemometer was used to obtain fluctuations of the virtual temperature, T_v', directly from the sonic signals; these fluctuations were correlated with the measured fluctuations in the vertical-velocity component to obtain the flux. In the second arrangement, a single-component sonic anemometer's output was correlated with the temperature signal from a thermocouple. Because the water vapor fluxes were low during the comparison period, $w'T'$ and $w'T_v'$ from the two sets of instruments are directly comparable, and the results are quite good.

The anticipated differences in the sensible- and latent-heat fluxes over the farm and steppe areas were consistently found by both airborne and ground-based instruments. Figure 3 shows an example of sensible- and latent-heat fluxes measured over a wheat field and over the steppe during 11–12 June. The relative roles of the fluxes are essentially reversed over the two surfaces; that is, over the wheat, the latent-heat flux is much larger than the sensible-heat flux, while over the steppe the opposite is true. Over the irrigated farmland, measured latent-heat fluxes were as high as 500 W m^{-2}, with sensible-heat fluxes on the order of 100–200 W m^{-2}.

Mean latent-heat and sensible-heat fluxes were calculated for the shrub (four sites) and grass (five sites) communities, and examples for three consecutive days are presented in Fig. 4. Mean maximum daily sensible-heat fluxes for both communities ranged from 270 to 450 W m^{-2}, while for latent-heat fluxes the maxima were between 45 and 80 W m^{-2}. There was no discernible effect of vegetative cover on the mean sensible-heat fluxes; inspection of the daily flux values

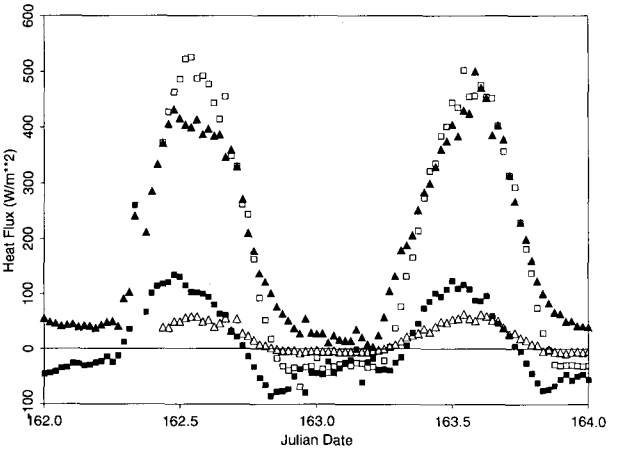

FIG. 3. Sensible- and latent-heat fluxes over steppe and irrigated wheat field for 11–12 June 1991. Open symbols are values for steppe, and filled symbols are for farmland. Squares denote sensible-heat values; triangles indicate latent-heat values.

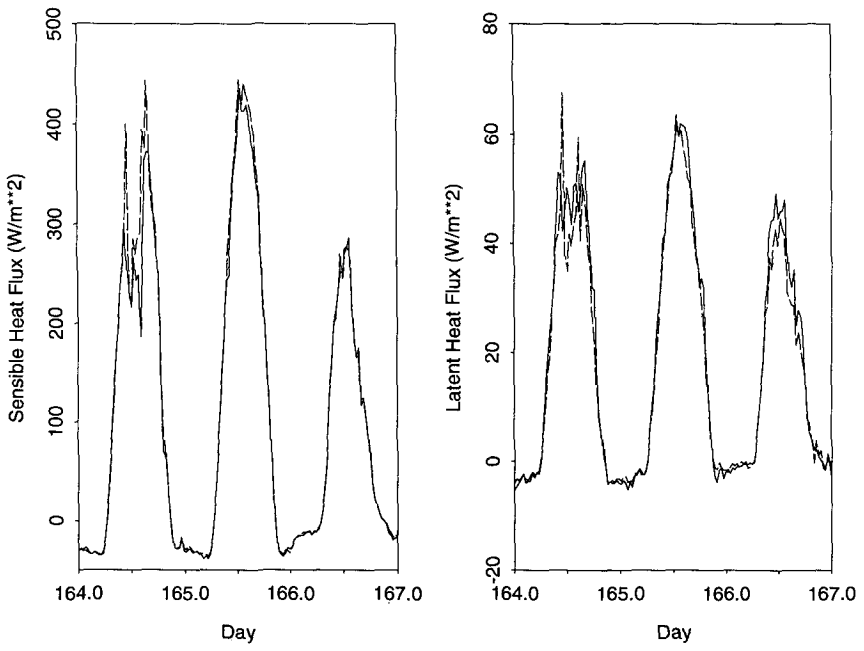

FIG. 4. Sensible- and latent-heat fluxes in shrub (solid lines) and grass (dashed lines) communities; note the different ranges on the *y* axes.

for each site showed that these fluxes were remarkably uniform among the sites. However, the latent-heat flux from the bitterbrush site was significantly higher than over the other shrub sites. This trend cannot be explained by the effect of soil moisture, which tended to be lower at this site. Although the overall vegetative cover on this site was similar to the other shrub sites (14%), the dominant shrub species (bitterbrush) has a larger growth form and higher green biomass per shrub than the rabbitbrush growing on the other shrub sites. The potentially higher biomass per unit ground area and the deeper rooting depth (likely with a larger shrub and resulting in the vegetation accessing soil moisture deep in the profile) could account for the higher evapotranspiration from this site. Other factors that may relate to site differences, such as soil texture, are being evaluated.

During the measurement period, there was almost no precipitation, and the vegetation showed little activity. Thus, flux differences between different plant communities were smaller than might have been the case earlier in the spring. In the farm area, the different crop types, growing periods, and irrigation schedules resulted in more variability. In particular, unseasonably cool weather caused late development in the corn so that the corn canopy was sparse, more soil was exposed, and a greater proportion of the available radiative energy appeared as sensible-heat fluxes over corn compared with other crops. Figures 5 and 6 show examples of the variation of sensible- and latent-heat fluxes over the steppe and various irrigated surfaces for 14 June. (As noted earlier, the maximum latent-heat values in the steppe were about an order

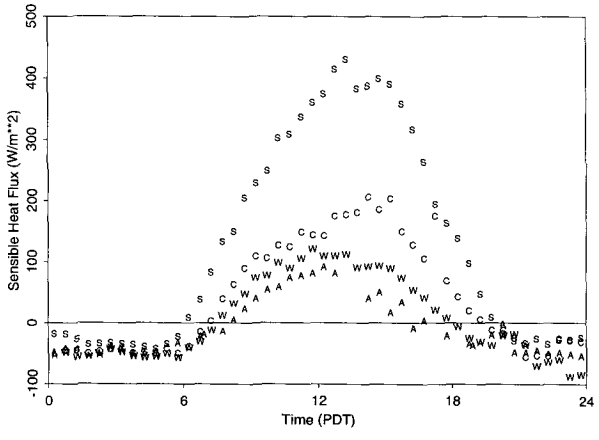

FIG. 5. Sensible-heat fluxes measured with eddy-correlation stations over alfalfa (A), wheat (W), corn (C), and steppe (S) on 14 June 1991.

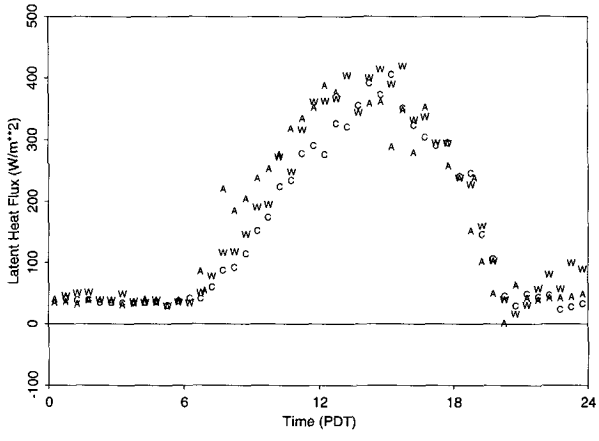

FIG. 6. Latent-heat fluxes measured with eddy-correlation stations over alfalfa (A), wheat (W), and corn (C) on 14 June 1991.

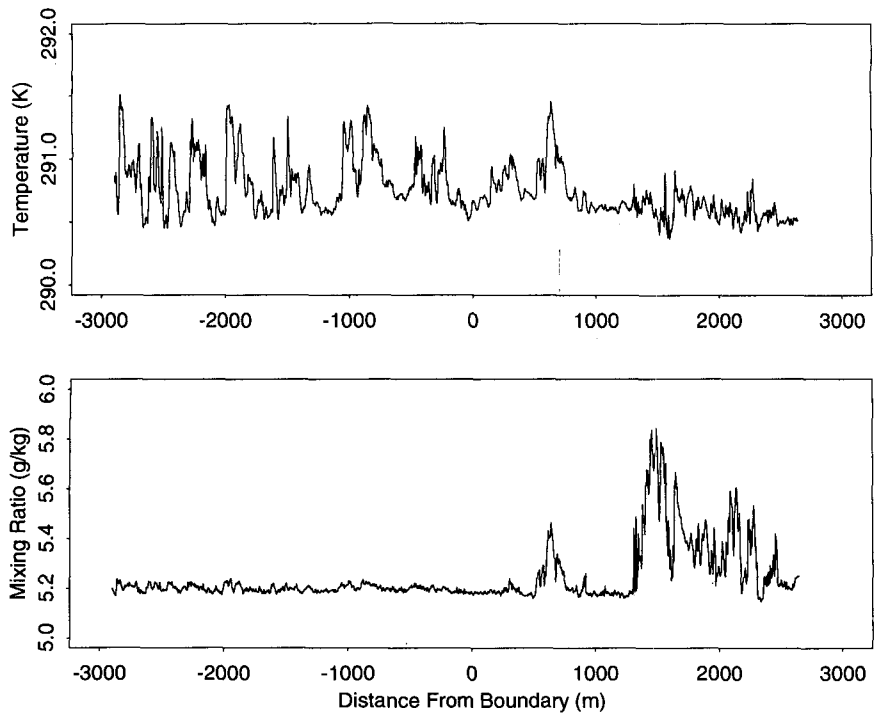

FIG. 7. Temperature and mixing-ratio values measured by the airplane in a transect from the steppe to the farm, 15 June 1991.

of magnitude smaller than the maximum sensible-heat values.) While there are variations over the farm, they are small compared to the differences between the farm and the steppe.

Time-series plots of temperature and mixing-ratio measurements from the aircraft show significant differences between flight segments over the steppe and farm. In the data shown in Fig. 7, obtained on 15 June, there is a noticeable lag from the time the aircraft passes from the steppe region to its first encounter with the internal boundary layer generated over the farm. In the subsequent path over the farm, the temperature fluctuations are strongly damped and the water vapor fluctuations strongly enhanced compared to values found over the steppe. Flight altitudes for this transect were 12 m AGL over the farm and 14 m AGL over the steppe.

Figure 8 shows a comparison of fluxes of latent heat, obtained over the steppe and the farm with the aircraft and with surface-based instruments on 14 June. For the aircraft measurements, fluxes were obtained from covariances computed over pathlengths of 4.5 km. Flight altitudes ranged between 11 and 20 m AGL. Each triangular symbol in the figure represents the value obtained from a single 4.5-km segment; analyses of the data using various pathlengths are continuing. On the same day, differences in the surface radiating temperatures, air temperatures, and wind speeds at flight altitudes over the steppe and farm, as measured by the aircraft, are also evident (Fig. 9). An emissivity of 0.95 has been assumed to obtain the ground temperatures. The slight differences in wind speed are consistent with the tendency to develop a "farm breeze" circulation from the cooler agricultural area to the warmer steppe. On this day the ambient winds were too strong to allow an organized flow from the farm to the steppe; on another occasion a shallow (200-m-deep) farm breeze from the irrigated region to the steppe was evident in the tethered-balloon data.

Data from the tethered-balloon flights also show markedly different temperature structures over the hotter and cooler regions. There are also some variations in the wind speeds, particularly near the surface, although the effects on the wind are more ambiguous. On at least one day, when the ambient winds near the surface were only 2–3 m s^{-1}, there was evidence for a shallow convective upslope flow over the steppe toward the higher terrain to the south.

Figure 10 illustrates sodar intensity profiles on the morning of 18 June, obtained simultaneously over the steppe and a potato field near the wet–dry transition

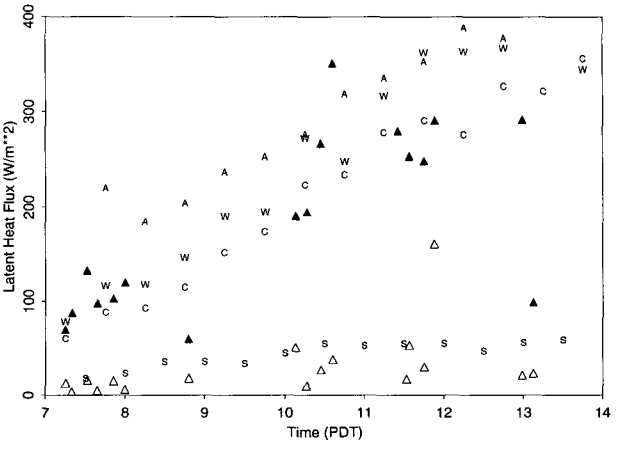

FIG. 8. Latent-heat fluxes measured by surface stations over alfalfa (A), wheat (W), corn (C), and the steppe (S), and by the airplane over the farm (filled triangles) and over the steppe (open triangles), 14 June 1991.

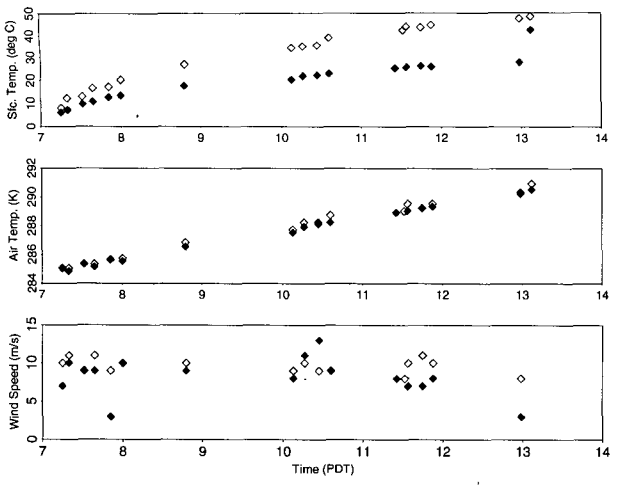

FIG. 9. Surface radiating temperatures, air temperatures, and wind speeds measured by the aircraft over the farm (filled diamonds) and over the steppe (open diamonds), 14 June 1991.

zone. On this day, winds were from the northeast and the skies were cloudy. Close examination shows an increased amount of structure above 50 m in the profile over the potatoes. The minisodar at this site "sees" near-surface profiles representative of potatoes and irrigated fields nearby. The profile above 80 m may result from air that was originally representative of steppe to the northeast of the farm and has been modified during its passage above the irrigated fields. The sudden change in slope of the profile immediately above the near-surface layer represents the interfacial, or connecting, layer between the two sections. Because the slopes of the profile below and above the matching zone are nearly the same and characteristic of unstable conditions [$d\log(C_T^2)/d\log(z) = -4/3$], one can calculate a value for surface heat flux representative of those two air masses. In comparison, the profiles from the steppe site are relatively free of structure, with a –4/3 slope well above 100 m, because of the more vigorous mixing over the steppe. Figure 11 shows heat fluxes calculated from the minisodar profiles above and below 80 m. Note the much larger heat fluxes calculated over the steppe compared to those found over the potatoes. Note also that the "elevated" profile above the potatoes represents some measure of a heat flux representative of both sites. The sharp increase in heat flux around noon over the potatoes corresponds to a strong increase in net radiation, which apparently resulted from a break in the cloud cover at this time.

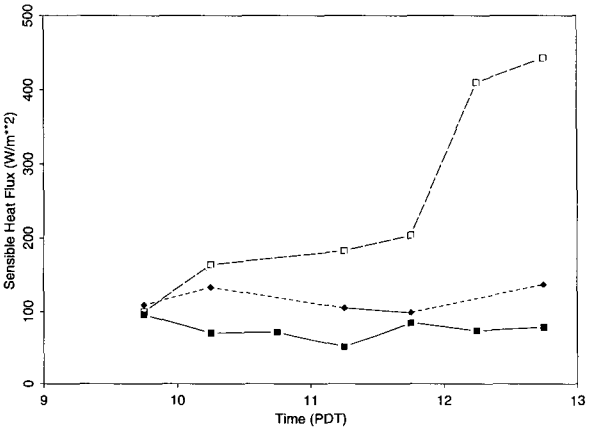

FIG. 11. Sensible-heat flux values derived from the minisodar intensity profiles for a potato field (filled squares) and the steppe (open squares) on 18 June 1991. The diamonds are derived from the "potato" profile values above 80 m.

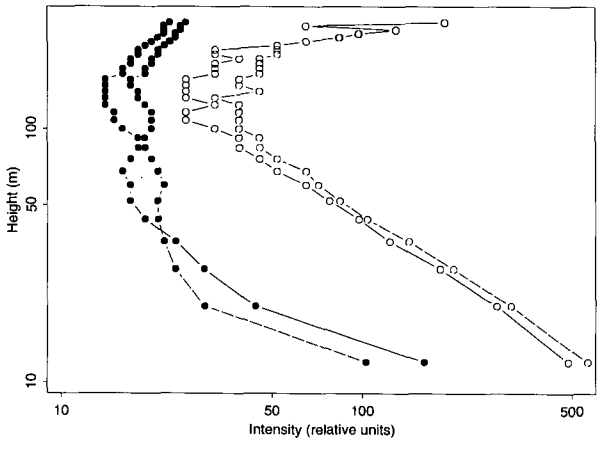

FIG. 10. Minisodar intensity profiles over potatoes (filled circles) and the steppe (open circles) at 0915 (solid lines) and 1015 (dashed lines) PDT on 18 June 1991.

Preliminary values of heat flux for 10 June calculated from the laser anemometer data over the farm area are illustrated in Fig. 12. The decrease of the heat flux above both the potato field and the combined path (potatoes and corn) after 1015 PDT is most likely due to the sprinkler system that was operating upwind in the potato field at this time. Around 1400 PDT the laser paths were enveloped by the sprinkler pattern, and no data were available for two half-hour sampling periods. The potato field was irrigated more regularly than the corn field during the experiment, and the effective leaf-area index of the potatoes was much greater. One would thus anticipate that the ratio of latent- to sensible-heat fluxes would be larger for the potato field than for the corn field. Indeed, the C_n^2 values from the laser anemometer path in the potatoes were regularly less than from the path in the corn, consistent with such an expectation. The combined path across both

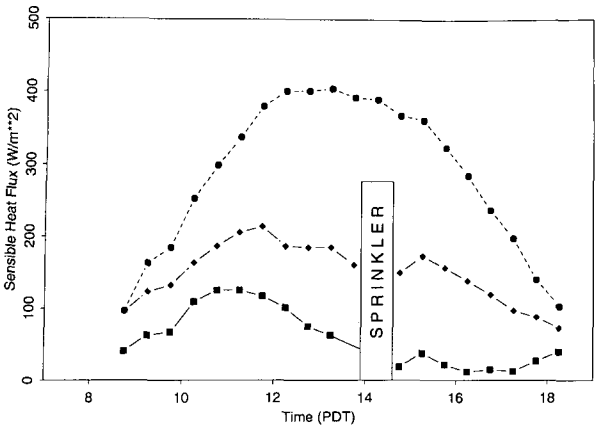

FIG. 12. Sensible-heat fluxes derived from optical scintillation measurements over potatoes (squares), corn (circles), and a corn–potato mix (diamonds) on 10 June 1991.

crops usually indicated an intermediate value of C_n^2, but the analysis of the values is complicated because the path included a dry, bare segment (an access road about 10 m wide) between the fields.

Figure 13 shows values of the horizontal wind convergence, estimated from the triangular array of anemometers in the steppe, and vertical-velocity values at 35 m obtained from a minisodar located near the middle of the triangle. On 10 June, the winds were predominantly from the north, which results in positive wind components along the optical path represented in the figure. On 16 June, the wind direction was from the southwest, giving negative values for the same path. As noted earlier, there is a gentle upwards slope from the Columbia River to the south, and a comparison of the convergence and vertical-velocity values for the two days shows an apparent effect of topography. Winds from the southwest were associated with downward vertical velocities and net divergence at the triangular array, while winds from the north had the opposite effect. The presence of regions of local convergence and divergence may complicate the interpretation of aircraft-derived fluxes.

6. Summary and future analyses

An experiment to measure the effects on the atmospheric boundary layer of sharply contrasting surface fluxes of sensible and latent heat has been carried out. The measurements were made with an extensive array of surface-based eddy-correlation and Bowen-ratio stations, an instrumented aircraft, sodars, tethered balloons, and optical wind and turbulence sensors. Extensive supporting data on soil and vegetation characteristics were collected concurrently.

Analyses show the expected large differences in surface fluxes between irrigated farmland and an adjacent steppe region. Sensible-heat fluxes in the steppe were two to three times larger than those in the irrigated areas; the latent-heat fluxes in the latter regions were often an order of magnitude larger than those in the steppe. Differences in flux values within the farm or steppe areas were generally signifi-

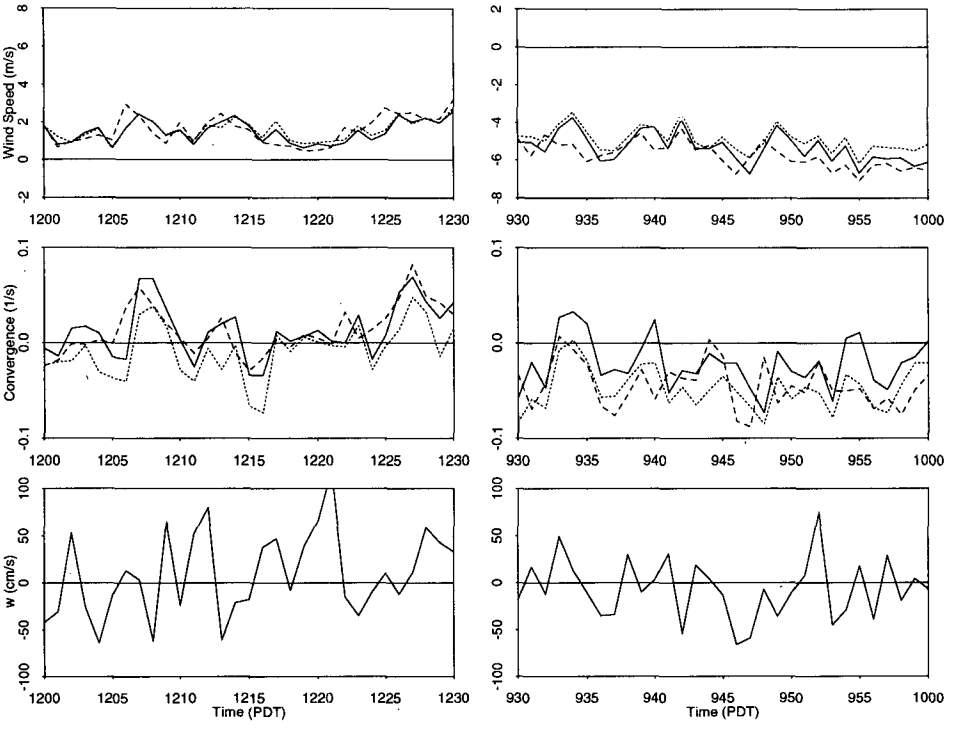

FIG. 13. Wind speeds, convergence, and *w* components of velocity measured on 10 June 1991 (left column) and 16 June 1991 (right column). In the top two figures of each column, the solid line is obtained from laser anemometer data, the fine dashed line from the saturation resistant optical array, and the coarse dashed line from anemometers located at the two ends of an optical path.

cantly smaller than the differences between the two regions.

There is evidence of differences in the properties of the overlying boundary layers in the two regions as well. Future research will concentrate on identifying and quantifying these differences and relating them to variations in the surface fluxes. We will also test one or more parameterizations used in GCMs to evaluate their usefulness over inhomogeneous surfaces and assess what modifications might be appropriate. Numerical mesoscale models will be applied to simulate the observations and to extend the range of conditions that can be studied.

Acknowledgments. This work was supported, in part, by the U.S. Department of Energy under Contracts DE-AC06-76RLO 1830, W-31-109-ENG-38, and W-7405-ENG-36. We would like to express our appreciation to the U.S. Navy for their cooperation in providing us access to the Naval Weapons Systems Training Facility and to the Boeing Agri-Industrial Company for granting access to land under their jurisdiction. Finally, we would like to thank Mr. Frank Lamb of Eastern Oregon Farming Co. for his cooperation and assistance during the course of our experiment.

References

André, J. -C., P. Bougeault, and J.-P. Goutorbe, 1990: Regional estimates of heat and evaporation fluxes over non-homogeneous terrain. Examples from the HAPEX-MOBILHY programme. *Bound.-Layer Meteor.*, **50,** 77–108.

Auble, D. L., and T. P. Meyers, 1992: An open path, fast response infrared absorption gas analyzer for H_2O and CO_2. *Bound.-Layer Meteor.*, **59,** 243–256.

Avissar, R., and R. A. Pielke, 1989: A parameterization of heterogeneous land surfaces for atmospheric numerical models and its impact on regional meteorology. *Mon. Wea. Rev.*, **117,** 2113–2136.

Barnes, F.J., D. Cooper, W. Porch, K.E. Kunkel, L. Hipps, and E. Swiatek, 1992: Variability of surface fluxes over a heterogeneous semi-arid grassland. *3rd Symp. on Global Change Studies,* Atlanta, GA, Amer. Meteor. Soc., 63–67.

Claussen, M., 1990: Area-averaging of surface fluxes in a neutrally stratified, horizontally inhomogeneous atmospheric boundary layer. *Atmos. Environ.*, **24A,** 1349–1360.

Coulter, R.L., W. Gao, T.J. Martin, J.D. Shannon, J.C. Doran, J.M. Hubbe, and W.M. Shaw, 1992: Evolution of the lower planetary boundary layer over strongly contrasting surfaces. *3rd Symp. on Global Change Studies,* Atlanta, GA, Amer. Meteor. Soc. 68–72.

Crawford, T., R.T. McMillen, and R.J. Dobosy, 1990: Development of a "generic" mobile flux platform with demonstration on a small airplane. NOAA Tech. Memo. ERL ARL-184, 81 pp.

Department of Energy, 1990: Atmospheric radiation measurement program plan, DOE/ER-0441. [Available from National Technical Information Service, U.S. Department of Commerce, Springfield, Virginia.]

Hall, F.G., B.J. Markham, J.R. Wang, and F. Huemmerich, 1990: FIFE results overview. *Symp. on FIFE,* Anaheim, California, Amer. Meteor. Soc., 17–24.

Kustas, W. P., D. C. Goodrich, M. S. Moran, S. A. Amer, L. B. Bach, J. H. Blanford, A. Chehbouni, H. Claassen, W. E. Clements, P. C. Doraiswamy, P. Dubois, T. R. Clarke, C. S. T. Daughtry, D. I. Gellman, T. A. Grant, L. E. Hipps, A. R. Huete, K. S. Humes, T. J. Jackson, T. O. Keefer, W. D. Nichols, R. Parry, E. M. Perry, R. T. Pinker, P. J. Pinter, Jr., J. Qi, A. C. Riggs, T. J. Schmugge, A. M. Shutko, D. I. Stannard, E. Swiatek, J. D. van Leeuwen, J. van Zyl, A. Vidal, J. Washburne, and M. A. Weltz, 1991: An interdisciplinary field study of the energy and water fluxes in the atmosphere-biosphere system over semiarid rangelands: Description and some preliminary results. *Bull. Amer. Meteor. Soc.* **72,** 1683–1705.

Mahrt, L., 1987: Grid-averaged surface fluxes. *Mon. Wea. Rev.*, **115,** 1550–1560.

Noilhan, J., and S. Planton, 1989: A simple parameterization of land surface processes for meteorological models. *Mon. Wea. Rev.*, **117,** 536–549.

Porch, W., F. J. Barnes, M. Buchwald, W. Clements, D. Cooper, D. Hoard, J. C. Doran, J. M. Hubbe, W. Shaw, R. L. Coulter, T. J. Martin, and K.E. Kunkel, 1992: Spatially averaged heat flux and convergence measurements at the ARM regional flux experiment. *3rd Symp. on Global Change Studies,* Atlanta, GA, Amer. Meteor. Soc., 125–131.

Rabin, R. M., S. Stadler, P. J. Wetzel, D. J. Stensrud, and M. Gregory, 1990: Observed effects of landscape variability on convective clouds. *Bull. Amer. Meteor. Soc.*, **69,** 272–280.

Stull, R. B., 1988: *An Introduction to Boundary Layer Meteorology.* Kluwer Academic Publishers, 666 pp.

Wyngaard, J. C., and S. F. Clifford, 1978: Estimating momentum, heat and moisture fluxes from structure parameters. *J. Atmos. Sci.*, **35,** 1204–1211.